Taguchi-based determination of double-ellipsoidal heat source parameters for numerical simulations of GMAW process

Mišo Bjelić[1*], Mladen Rasinac[1], Aleksandra Petrović[1], Marina Ivanović[1], Jovana Perić[1]
[1]Faculty of Mechanical and Civil Engineering in Kraljevo, University of Kragujevac, Kraljevo (Serbia)

The results of the application of welding simulation models are highly dependent on the input parameters, particularly on the parameters of the heat source model. In this study, a method for determining the heat source parameters for a three-dimensional quasi-stationary heat transfer model for gas metal arc welding is presented. The commonly used double-ellipsoidal heat source has five input parameters, the values of which are mainly chosen based on the researcher's experience. This approach is a common source of error; to estimate these values, we applied a calibration procedure using the Taguchi method with combined objective function based on weld geometry. The simulation results show that the Taguchi method can be successfully used to determine the heat source parameters.

Keywords: Numerical simulation, Taguchi method, Heat source model, GMAW

1. INTRODUCTION

Welding thermal cycle caused by localized heat source has dominant influence on mechanical properties, deformations and residual stresses of weld and nearby metal. Modeling of heat transfer during welding is of great importance in order to understand these influences. Today’s models describe not only conduction but also convection, fluid flow, free surface deformation and arc physics. Key to successful simulation of heat transfer during welding is an adequate heat source model. There is a whole variety of heat source models used today, from simple ones, such as Rosenthal’s and Rykalin’s [1,2]to the complex models that describe convection in the weld pool, fluid flow, free surface deformation and arc physics. One of the most frequently used models is Goldak’s double-ellipsoidal model [3] with the volumetric power density distribution, Fig. 1. Five input parameters that define this model are arc efficiency, and four semi-axes of the front and rear ellipsoid. The power of the heat source is distributed, Eqs. (1-3), between the front and rear ellipsoids in a ratio that corresponds to values of parameters $f_f=2a_f/(a_f+a_r)$ and $f_r=2a_r/(a_f+a_r)$ [4].

Values of these input parameters vary significantly, as in the case of arc efficiency. Depending on the type of welding process and shielding gas, arc efficiency can vary between 0.8 and 0.88, as found by DuPont and Marder [5] in case of GMAW process with Ar shielding. Haelsig and Mayr [6] found that arc efficiency has a value, between 0.69 in case of spray arc to the 0.85 in case of short arc shielding. With pulsed transfer, arc efficiency ranges from 0.68 to 0.72 as found by Joseph et al [7]. For the other four heat source parameters, Goldak et al suggested that the values of b_h and c_h should be taken from an experimental cross-section of the weld while the values of a_f and a_r should be equal to b_h and $2b_h$, respectively. In absence of experimental cross section, values of these four parameters should be calculated using Christensen formulae [8]. As for the values of the parameters a_f and a_r, they can vary from $a_r/a_f=1.22$ [9] and up to $a_r/a_f=4$ [10]. Value of parameter a_f is often taken to be equal to c_h [10] or b_h [11]. Guided by Goldak’s recommendation, Nasiri and Enzinger used the parameters of a double-ellipsoidal heat source that was approximately 10% smaller than the actual weld geometry [12].

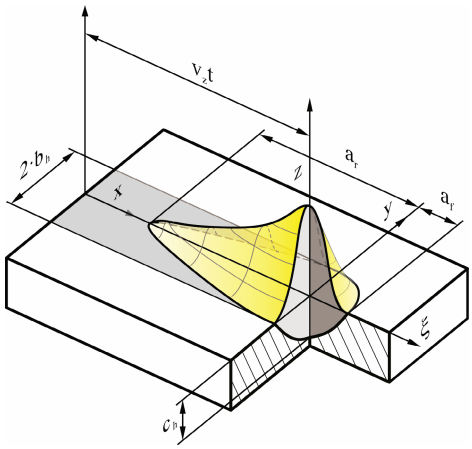

Figure 1: Goldak’s double-ellipsoidal heat source

$$q_f(x,y,z)=\frac{6\sqrt{3}f_fQ}{a_fb_hc_h\pi\sqrt{\pi}}e^{-3\frac{x^2}{a_f^2}}e^{-3\frac{y^2}{b_h^2}}e^{-3\frac{z^2}{c_h^2}} \quad (1)$$

$$q_r(x,y,z)=\frac{6\sqrt{3}f_rQ}{a_rb_hc_h\pi\sqrt{\pi}}e^{-3\frac{x^2}{a_r^2}}e^{-3\frac{y^2}{b_h^2}}e^{-3\frac{z^2}{c_h^2}} \quad (2)$$

$$Q=\eta UI \quad (3)$$

The determination of the values of these five parameters is essential for obtaining accurate results from the welding heat transfer model. This goal can be achieved using inverse modeling, that is, minimizing the error between simulated and experimental values of the weld cross-section geometry [11,12]. For this purpose, the simulation model is often combined with an optimization method or the simulation model is replaced with a metamodel to reduce the required computational time [15]. This approach implies that the model being calibrated is supplied with input data until the simulation results match the experimental ones. However, random assignment of values to input parameters usually implies a large number of necesary simulations, which results in a very long time required for model calibration.

*Corresponding author: Dositejeva 19, 36000 Kraljevo, Serbia, bjelic.m@mfkv.kg.ac.rs

To avoid this, we used the Taguchi method to systematize and reduce the number of combinations of input data. These values were used as input parameters for a double-ellipoidal heat source. Thus, we were able to determine the optimal values of the heat source parameters that minimized the error between the simulated and experimental values of the weld penetration depth and weld bead width.

2. MODEL OF HEAT TRANSFER

Nonstationary partial differential equation (4) [11] can be used to describe heat transfer during welding, where ρ, cp, and λ are the density, specific heat capacity, and thermal conductivity, respectively, and L and q_l are the latent heat of melting/solidification and volumetric heat source, respectively. There are difficulties associated with an analytical solution to this type of equation due to nonlinearities in the material's physical properties. The complexity of the boundary conditions and the model of the heat source contributes to these difficulties.

$$\rho c_p \frac{\partial T}{\partial t} = \lambda\left(\frac{\partial^2 T}{\partial x^2}+\frac{\partial^2 T}{\partial y^2}+\frac{\partial^2 T}{\partial z^2}\right)-\rho L\frac{\partial f_{liq}}{\partial t}+q_l \qquad (4)$$

The latent heat of melting/solidification was calculated using the liquid phase fraction in the mushy zone between the solidus temperature T_{sol} and liquidus temperature T_{liq}, as shown in (5).

$$f_{liq}=\begin{cases}0 & for \quad T \le T_{sol}\\ \dfrac{T-T_{sol}}{T_{liq}-T_{sol}} & for \quad T_{sol}<T<T_{liq}\\ 1 & for \quad T \ge T_{liq}\end{cases} \qquad (5)$$

It is possible to transform (4) for a constant welding speed v_w into a quasi-steady state (7). This type of transformation requires the application of a moving coordinate system ξyz, as shown in Fig. 1. The relationship between these two coordinate systems is defined by (6).

$$\xi = x - v_w t \qquad (6)$$

Now, the heat transfer equation in the moving coordinate system can be written as:

$$-v_w\left(1+\frac{L}{c_p}\frac{\partial f_{liq}}{\partial T}\right)\frac{\partial T}{\partial \xi}=\frac{\lambda}{\rho c_p}\left(\frac{\partial^2 T}{\partial \xi^2}+\frac{\partial^2 T}{\partial y^2}+\frac{\partial^2 T}{\partial z^2}\right)+q_l \qquad (7)$$

Equation (7) is solved in MATLAB iteratively using the multigrid and SOR finite difference methods.

3. EXPERIMENTAL PROCEDURE

An experimental specimen of 300x150x5.3 mm was used for calibration purposes. The base material for the specimen was P355GH steel, with the chemical composition listed in Table 1.

OK Autrod 12.50 uncoated wire with a diameter of 1.2 mm and chemical composition listed in Table 2 was used as filler material. A two-component mixture of 82% Ar and 18% CO2 was utilized as a shielding gas.

Table 1: Chemical composition of base material

C	Si	Mn	Nb	P	S
0.20	0.19	1.45	0.014	0.016	0.062

Welding was performed on one specimen using an ARC Mate 100iC welding robot and Migatronic Sigma Galaxy 400 power supply.

Table 2: Chemical composition of filler material

C	Si	Mn	P	S
0.08	0.58	1.06	0.009	0.01

Using the welding parameters listed in Table 3, a single-pass bead-on-plate weld was made along the specimen's centerline.

Table 3: Welding parameters

Voltage [V]	Current [A]	Welding speed [mm/s]	Wire feed rate [m/min]	Wire diameter [mm]	Gas flow [l/min]
21.2	208	8	5.2	1.2	12

In order to determine the dimensions of the weld geometry, a macrograph section of the weld bead was prepared after welding (Fig. 2).

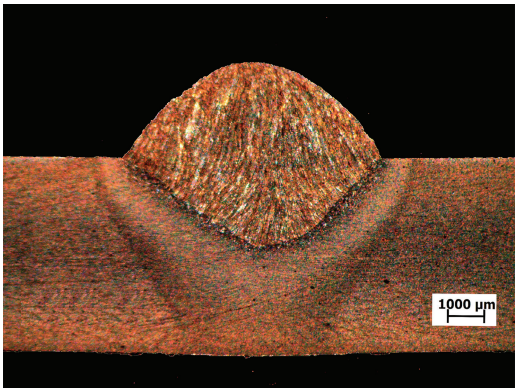

Figure 2: Macrograph of weld bead

The width and penetration depth of the weld bead were measured, as shown in Fig. 3. The measurements were conducted using an STEMI DV-4 stereo microscope equipped with an AxioCam Erc 5S camera.

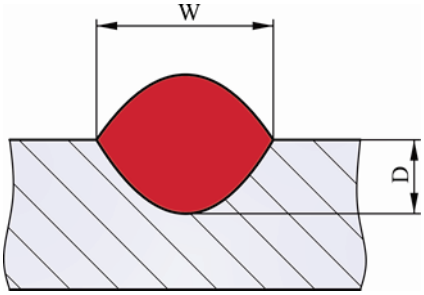

Figure 3: Measured weld geometry

The values of the measured dimensions are listed in Table 4.

Table 4: Measured weld dimensions

W [mm]	D [mm]
7.2	2.4

4. TAGUCHI METHOD

Developed by Genichi Taguchi, the Taguchi method is a statistical approach for optimizing the quality of products and processes. The method is widely used in engineering and manufacturing to enhance robustness and reliability while minimizing the effects of variability. Essentially, the Taguchi method involves identifying and controlling the factors that contribute to system variability. A set of factors can be categorized in three categories: control factors, that is, design parameters or controllable variables, noise factors, and signal factors, that is, response variables.

Taguchi method uses the signal-to-noise ratio (S/N) to evaluate a product or process' performance characteristics. The signal-to-noise ratio implies three categories of performance characteristics: lower-the-better, higher-the-better, and nominal-the-better. A lower-the-better characteristic is used when it is necessary to minimize the response. It can be expressed as (8):

$$S/N = -10\log\left(\frac{1}{n}\sum_{i=1}^{n} Y_i^2\right) \tag{8}$$

When the response must be maximized, the larger-the-better characteristic is used (9),

$$S/N = -10\log\left(\frac{1}{n}\sum_{i=1}^{n}\frac{1}{Y_i^2}\right) \tag{9}$$

When considering the nominal-the-best characteristic, there is a target or desired value for the response variable. The S/N ratio is calculated as (10):

$$S/N = -10\log\left(\frac{1}{n}\sum_{i=1}^{n}\left(\mu - Y_i\right)^2\right) \tag{10}$$

where n is the number of observed values, in this case, the number of objective functions, Yi is the value of the observed characteristic, that is, the value of the objective function, and μ is the target value or the nominal value. For all three performance characteristics, a higher S/N ratio corresponded to better performance characteristics.

Calculating the S/N ratio for each experiment or test allows a comparison between different parameter settings and identification of the combination providing the highest S/N ratio.

The observed characteristic is defined by (11)

$$Y = \left(1 - W_j^{sim}/W^{\exp}\right)^2 + \left(1 - D_j^{sim}/D^{\exp}\right)^2 \tag{11}$$

where W_j^{sim} and D_j^{sim} are the values of the simulated weld bead width and penetration depth, respectively; W_{exp} and D_{exp} are the measured values of the specimen weld bead width and penetration depth, respectively; j is the number of simulation runs. The chosen performance characteristic defined by the S/N ratio is, in this case, lower-the-better.

The minimal degrees of freedom required to choose the right experimental plan (dof_{exp}) depends on the number of factors (i) and degrees of freedom for each factor (dof^{fact}), as well as the factor interactions (dof^{int}), and is defined by (12):

$$dof_{\exp} = \sum_{i=1}^{n} dof_i^{fact} + \sum_{j=1}^{m} dof_j^{\text{int}} \tag{12}$$

In this case, each of the five factors was considered at five levels, as shown in Table 5.

Table 5: Heat source parameters and their levels

Parameter	Level					dof_{fact}
	1	2	3	4	5	
η	0.55	0.65	0.75	0.85	0.95	4
a_f/a_{fexp}	0.8	0.9	1	1.1	1.2	4
a_r/a_{rexp}	0.8	0.9	1	1.1	1.2	4
b_h/b_{hexp}	0.8	0.9	1	1.1	1.2	4
c_h/c_{hexp}	0.8	0.9	1	1.1	1.2	4

Bearing in mind that the interactions between factors were not considered, minimal dof_{exp}=20. Based on this, we chose the Taguchi's $L_{25}(5^6)$ orthogonal array, as shown in Table 6.

Table 6: $L_{25}(5^6)$ OA and parameters values

Run	η	a_f/a_{fexp}	a_r/a_{rexp}	b_h/b_{hexp}	c_h/c_{hexp}
1.	0.65	1.2	0.8	0.9	1
2.	0.65	1	1.1	1.2	0.8
3.	0.55	1.1	1.1	1.1	1.1
4.	0.75	0.8	1	1.2	0.9
5.	0.55	1	1	1	1
6.	0.55	1.2	1.2	1.2	1.2
7.	0.95	1	0.9	0.8	1.2
8.	0.75	0.9	1.1	0.8	1
9.	0.65	0.9	1	1.1	1.2
10.	0.75	1.1	0.8	1	1.2
11.	0.75	1.2	0.9	1.1	0.8
12.	0.95	1.1	1	0.9	0.8
13.	0.95	0.8	1.2	1.1	1
14.	0.65	1.1	1.2	0.8	0.9
15.	0.55	0.8	0.8	0.8	0.8
16.	0.85	1.1	0.9	1.2	1
17.	0.85	1	0.8	1.1	0.9
18.	0.85	1.2	1	0.8	1.1
19.	0.85	0.9	1.2	1	0.8
20.	0.75	1	1.2	0.9	1.1
21.	0.55	0.9	0.9	0.9	0.9
22.	0.85	0.8	1.1	0.9	1.2
23.	0.65	0.8	0.9	1	1.1
24.	0.95	0.9	0.8	1.2	1.1
25.	0.95	1.2	1.1	1	0.9

For each of the 25 combinations of double-ellipsoidal heat source parameters shown in Table 5, we performed a simulation run and obtained the simulated weld bead width and penetration depth for each combination. Table 7 lists the values of observed characteristic Y and its S/N ratio.

Table 7: Values of observed characteristics and S/N ratio

Run	W_s [mm]	D_s [mm]	W_{exp} [mm]	D_{exp} [mm]	Y	SN
1.	5.4	2.3	7.2	2.4	0.064236	23.84442
2.	6.1	1.9			0.066744	23.51178
3.	4.2	1.7			0.258681	11.74472
4.	6.4	2.3			0.014082	37.02684
5.	4.7	1.8			0.183063	14.74798

Run	W_s [mm]	D_s [mm]	W_{exp} [mm]	D_{exp} [mm]	Y	SN
6.	3.7	1.5	7.2	2.4	0.376929	8.474809
7.	6.1	3.2			0.134452	17.42864
8.	5.2	2.4			0.07716	22.2521
9.	5.2	2			0.104938	19.58132
10.	5.9	2.6			0.039545	28.05822
11.	6.7	2.4			0.004823	46.3345
12.	6.6	2.5			0.008681	41.22905
13.	6.7	2.7			0.020448	33.78718
14.	4.7	1.9			0.163966	15.70492
15.	4.7	1.9			0.163966	15.70492
16.	6.8	2.5			0.004823	46.3345
17.	6.9	2.6			0.008681	41.22905
18.	5.7	2.7			0.059028	24.57887
19.	6.4	2.3			0.014082	37.02684
20.	5.3	2.3			0.071373	22.92927
21.	4.7	1.8			0.183063	14.74798
22.	5.7	2.8			0.071181	22.95277
23.	5.3	2.2			0.076582	22.31749
24.	7.1	2.7			0.015818	36.01702
25.	6.5	2.5			0.011188	39.02474

The mean S/N ratios of the observed characteristic Y were calculated for each level of the heat source parameters and are listed in Table 8.

Table 8: Response table for S/N ratios of Y

Level	η	a_f	a_r	b_h	c_h
1	13.08	26.36	28.97	19.13	32.76
2	20.99	25.93	29.43	25.14	29.55
3	31.32	23.97	27.43	28.24	28.19
4	34.42	28.61	23.9	30.54	23.52
5	33.5	28.45	23.58	30.27	19.3
Delta	21.34	4.64	5.85	11.4	13.46
Rank	**1**	**5**	**4**	**3**	**2**

Based on the delta values in Table 8, it can be concluded that the heat-source parameters can be ranked based on their effect on the observed characteristic Y in the following descending order: $\eta > c_h > b_h > a_r > a_f$.

Figure 4 shows the effects of the heat source parameters on the mean S/N ratio of the observed characteristic Y. As previously mentioned, a higher S/N value corresponds to better performance of the observed characteristic. The combination of heat source parameters with the highest S/N ratio is considered optimal. In this case that values are η=0,85; a_f/a_{fexp} =1.1; a_r/a_{rexp} =0.9; b_h/b_{hexp} =1.1; c_h/c_{hexp} =0.8.

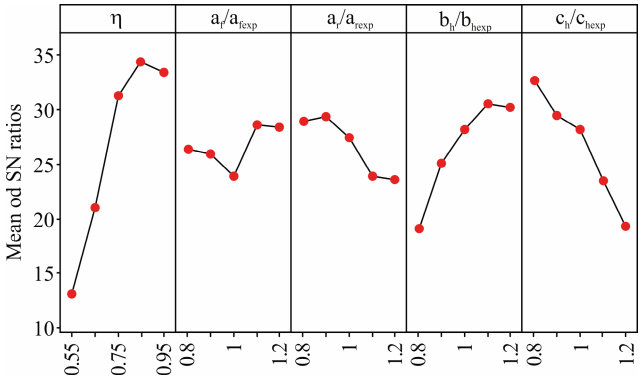

Figure 4: Main effects of heat source parameters

Because there was no experimental run with this set of heat source parameters, we performed an additional simulation run to confirm the results of the optimization. The results of the comparison between the simulated and experimental values of the weld geometry are shown in Table 9.

Table 9: Absolute and relative errors

Values	Parameter	
	W [mm]	D [mm]
Simulation	7	2.5
Experiment	7.2	2.4
Absolute error	0.2	0.1
Relative error	0.0278	0.0417

Figure 5 shows the simulated weld geometry compared with the experimental geometry.

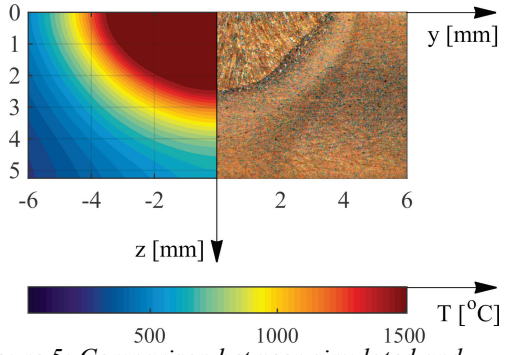

Figure 5: Comparison between simulated and experimental weld bead geometry

To investigate the effects of the heat source parameters on the observed characteristics, analysis of variance (ANOVA) was performed, and the results are listed in Table 10.

Table 10: Results of ANOVA for S/N ratios

Source	DF	SS	MS	F	p
Model	20	2961.36	148.07	12.90	0.0117
η	4	1725.92	431.48	37.6	0.002
a_f/a_{fexp}	4	74.5	18.62	1.62	0.325
a_r/a_{rexp}	4	153.58	38.39	3.35	0.134
b_h/b_{hexp}	4	447.52	111.88	9.75	0.024
c_h/c_{hexp}	4	559.84	139.96	12.2	0.016
Res. Err.	4	45.9	11.47		
Total	24	3007.25			

From Table 10, it can be seen that a model F-value of 12.90 implies the significance of the model. There is only a 1.17% chance that an F-value this large could occur due to noise. P-values less than 0.0500 indicate that the model terms are significant. In this case η, b_h, c_h are significant model terms which is consistent with results of previous analysis.

Analysis of variance allows us to evaluate the contribution of each parameter of the heat source to the mean S/N ratio of the observed characteristic Y. Those contributions are shown on Figure 6.

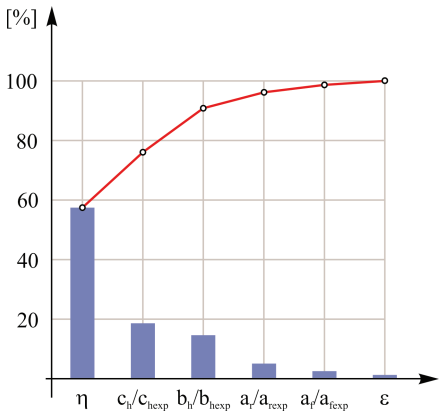

Figure 6: Pareto chart of heat source parameters contribution

The value of the parameter η was 0.85, which is consistent with the findings of DuPont et al. [3]. Parameter ch is 20% smaller, whereas parameter bh is 10% larger than the actual geometry. The relative error for the weld bead width was 2.8 while for the penetration depth was 4.2%.

5. SUMMARY AND CONCLUSIONS

As a means of improving the accuracy of our numerical model of three-dimensional heat transfer, we developed a calibration procedure for determining the input parameters of the double-ellipsoid heat source. The procedure was based on Taguchi's $L_{25}(5^6)$ OA design. As a result, this approach was found to be effective and reliable for accelerating the calibration process. Simulations based on the heat source parameters calculated using the calibration model demonstrate good agreement between simulated and actual weld geometry. The Taguchi-based calibration procedure is therefore demonstrated to be a reliable method for increasing the accuracy of simulation model output results.

ACKNOWLEDGEMENT

The authors wish to express their gratitude to the Ministry of Science, Technological Development and Innovation of the Republic of Serbia for support through contract No. 451-03-47/2023-01/200108.

LITERATURE

[1] D. Rosenthal, "The theory of moving sources of heat and its application to metal treatments", Transactions ASME, Vol. 43, pp. 849–866, (1946)

[2] N.N. Rykalin, "Calculations of thermal processes in welding", Mašgiz, Moscow (USSR), (1951)

[3] J. Goldak, A. Chakravarti and M. Bibby, "A new finite element model for welding heat sources", Metallurgical Transactions B, Vol. 15, pp. 299–305, (1984)

[4] C.S. Wu, "Welding thermal processes and weld pool behaviors", Taylor & Francis, Boca Raton-Florida (USA), 2011

[5] J.N. DuPont and A.R. Marder, "Thermal Efficiency of Arc Welding Processes", Welding Journal, Vol. 74, (1995).

[6] A. Haelsig and P. Mayr, "Energy balance study of gas-shielded arc welding processes", Welding in the World, Vol. 57, pp. 727–734, (2013)

[7] A. Joseph, D. Harwig, D.F. Farson and R. Richardson, "Measurement and calculation of arc power and heat transfer efficiency in pulsed gas metal arc welding", Vol. 8, pp. 400–406, (2013)

[8] N. Christensen, V. de L. Davies and K. Gjermundsen, "Distribution of temperatures in arc welding", British Welding Journal, Vol. 12, pp. 54–75, (1965)

[9] N. Moslemi, S. Gohari, B. Abdi, I. Sudin, H. Ghandvar, N. Redzuan, S. Hassan, A. Ayob and S. Rhee "A novel systematic numerical approach on determination of heat source parameters in welding process", Journal of Materials Research and Technology, Vol. 18, pp. 4427–4444, (2022)

[10] J.H. Chujutalli, M.I. Lourenço and S.F. Estefen, "Experimental-based methodology for the double ellipsoidal heat source parameters in welding simulations", Marine Systems and Ocean Technology, Vol. 15, pp. 110–123, (2020)

[11] G. Fu, J. Gu, M.I. Lourenco, M. Duan and S.F. Estefen, "Parameter determination of double-ellipsoidal heat source model and its application in the multi-pass welding process", Ships and Offshore Structures, Vol. 10, pp. 204–217, (2015)

[12] M.B. Nasiri and N. Enzinger, "Powerful analytical solution to heat flow problem in welding", International Journal of Thermal Sciences. Vol. 135, pp. 601–612, (2019)

[13] A. Kumar and T. DebRoy, "Guaranteed fillet weld geometry from heat transfer model and multivariable optimization", International Journal of Heat and Mass Transfer, Vol. 47, pp. 5793–5806, (2004)

[14] Y. Gu, Y.D. Li, Y. Yong, F.L. Xu and L.F. Su, "Determination of parameters of double-ellipsoidal heat source model based on optimization method", Welding in the World, Vol. 63, pp. 365–376, (2019)

[15] M.B. Bjelić, B.S. Radičević, K. Kovanda, L. Kolarik and A. V. Petrović, "Multi-objective calibration of the double-ellipsoid heat source model for GMAW process simulation", Thermal Science, Vol. 26, pp. 2081–2092, (2022)